

# Synthesis and Structure of a Bis(Double Helicate) and its Cryptatoclathrate\*\*

Rolf W. Saalfrank,\* Roland Harbig, Jochen Nachtrab, Walter Bauer, Klaus-Peter Zeller, Dietmar Stalke and Markus Teichert

**Abstract:** The structures of the hitherto unknown bis(double helicate) **10** and its cryptatoclathrate  $(10)_2 \cdot 2 \text{ THF}$  were unequivocally determined by X-ray diffraction. Bis(double helicate) **10** is formed in a one-pot synthesis starting from CH-acidic bis(tetrazolylmethyl ketone) **9** and  $\text{Zn}(\text{OAc})_2$ . The formation of racemic, homochiral **10** from  $[\text{Zn}_2\text{L}_2^3]$  fragments, which are formed in a self-assembly process, is governed by chiral self-recognition. According to NMR studies only **10** is present in solution.  $^{13}\text{C}$  CP/MAS NMR spectroscopy and X-ray analysis confirm aggregation of **10** with two molecules of THF to yield the inclusion compound  $(10)_2 \cdot 2 \text{ THF}$  in the solid state.

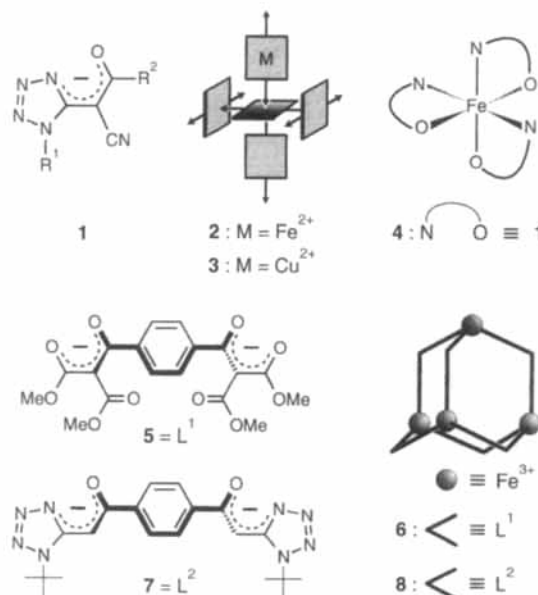
**Keywords**  
clathrates · cryptates · helicates · self-assembly · zinc complexes

## Introduction

Tetrazolylenolate ions **1** react with iron(II) and copper(II) ions to give coordination polymers **2**<sup>[1]</sup> and **3**<sup>[2]</sup> respectively. In the case of copper the 3D structure of the polymer has been established by X-ray crystallography.<sup>[2]</sup> However, with iron(III) ions the anions **1** yield mononuclear chelate complexes **4**.<sup>[1]</sup> In contrast, reaction of ligand **5** ( $= \text{L}^1$ , accessible from tetramethyl-2,2'-terephthaloyl dimalonate by double deprotonation) and iron(III) ions leads to the tetranuclear complex  $[\text{Fe}_4\text{L}_6^1]$  (**6**).<sup>[3, 4]</sup> Ligand **7** ( $= \text{L}^2$ ) combines the good complex-building properties of **1** towards iron(III) ions and the geometry of ligand **5**. Consequently, ligands **5** and **7** yield similar tetranuclear chelate complexes  $[\text{Fe}_4\text{L}_6^1]$  (**6**) and  $[\text{Fe}_4\text{L}_6^2]$  (**8**).<sup>[5]</sup> These supramolecular systems are formed exclusively by spontaneous self-assembly.<sup>[6]</sup>

## Results and Discussion

We were interested in studying the impact on the complex formation ability of the geometric changes when the *para*-phenylene spacer in ligand **7** was replaced with a *meta*-phenylene spacer. Accordingly we doubly deprotonated  $[\text{H}_2\text{L}^3]$  **9** with triethylamine and reacted the corresponding dianion  $\text{L}^{3-}$



with iron(III) chloride or zinc(II) acetate solution. The introduction of zinc(II) acetate makes triethylamine superfluous (for further details, see experimental part).

According to microanalyses and FAB MS data (FAB = fast atom bombardment), the composition of the products obtained is  $[\text{Fe}_2\text{L}_3^3]$ <sup>[5, 7]</sup> and  $[\text{Zn}_4\text{L}_4^3]$  (**10**), respectively.

The  $^1\text{H}$  and  $^{13}\text{C}$  NMR spectra of **10** do not unambiguously establish the structure of this complex. In order to characterize **10** unequivocally, we carried out an X-ray crystallographic structure analysis. According to this analysis, **10** is present in the crystal as a neutral tetranuclear bis(double helicate) that contains a molecular cavity<sup>[8]</sup> (Fig. 1). The core of **10** is formed by a distorted cuboid whose eight corners are occupied by alternating zinc and  $\mu_2$ -bound ketoxygen atoms. The faces (Zn-O-Zn-

[\*] Prof. Dr. R. W. Saalfrank, Dr. R. Harbig, Dipl.-Chem. J. Nachtrab, Priv.-Doz. Dr. W. Bauer  
Institut für Organische Chemie der Universität Erlangen-Nürnberg  
Henkestrasse 42, D-91054 Erlangen (Germany)  
Fax: Int. code + (9131)85-6864

Prof. Dr. D. Stalke, Dipl.-Chem. M. Teichert<sup>[1]</sup>  
Institut für Anorganische Chemie der Universität Würzburg (Germany)  
Prof. Dr. K.-P. Zeller<sup>[\*]</sup>  
Institut für Organische Chemie der Universität Tübingen (Germany)

[\*\*] "Adamantanoid Chelate Complexes", Part 6; for Part 5, see ref. [4].

[†] Single-crystal X-ray analysis.

[\*] FAB-mass spectroscopy.

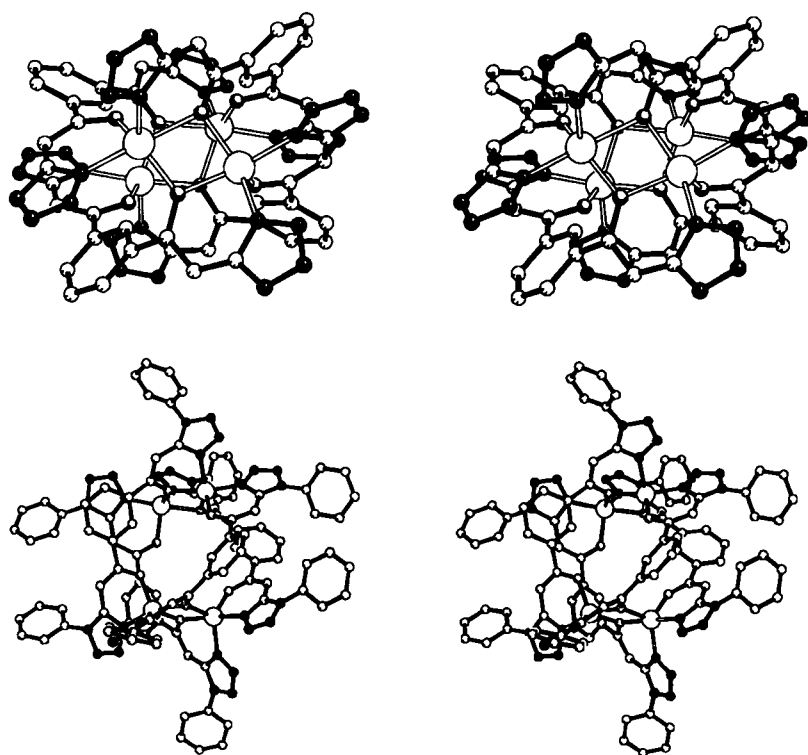


Fig. 1. Top: Stereoview of the crystal structure of bis(double helicate) **10** perpendicular to the Zn-O-Zn plane (nitrogen dark; oxygen shaded). For reasons of clarity, H atoms, phenyl groups and the solvent of crystallization (THF) are omitted (PLUTON [17]). Bottom: Stereoview of **10** (view parallel to the Zn-O-Zn plane, through the cavity; H atoms and THF molecules omitted).

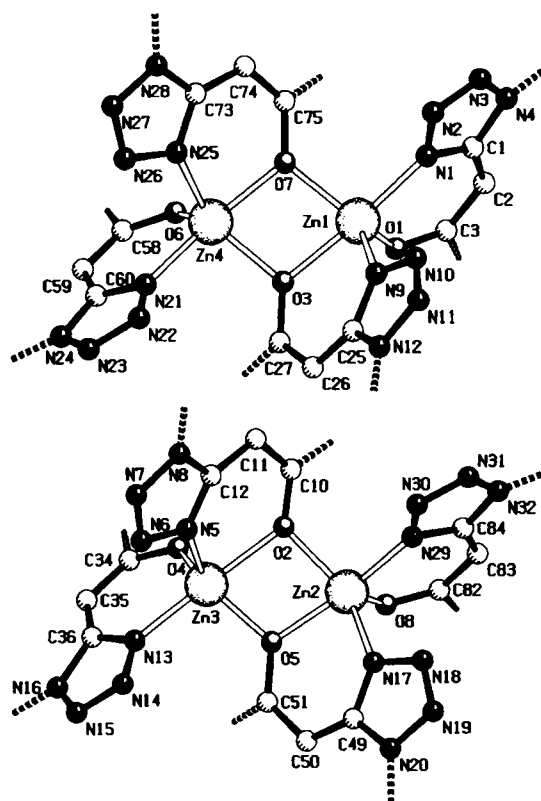
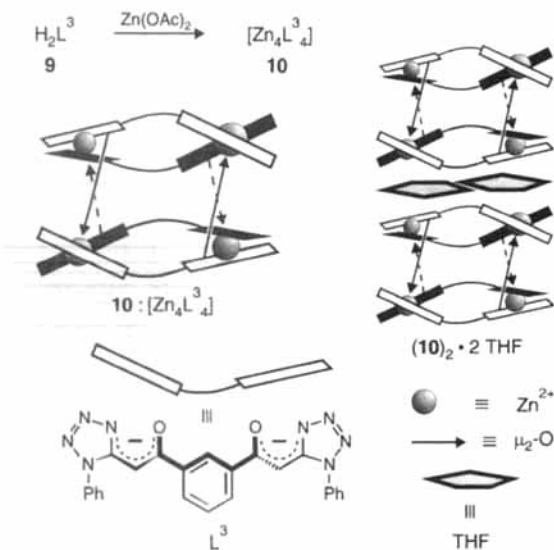


Fig. 2. Coordination spheres of  $Zn^{2+}$  ions in **10** (PLUTON [17]). Selected distances and angles are listed in Table 1.



O-) are offset by an angle of ca.  $45^\circ$ . Each zinc ion is bound to three ligands ( $N, \mu_1-O; N, \mu_2-O$ ; and  $\mu_2-O$ ) and is coordinated in a distorted trigonal bipyramidal manner (Fig. 2, Table 1). In detail, the three-dimensional structure of **10** results from linking two  $C_2$ -symmetric double helical<sup>[9]</sup> building blocks, each composed of two zinc ions and two ditope ligands  $L^3$ . Thus, each ligand is coordinated through one keto-oxygen atom  $\mu_1$  to a zinc ion. The two other  $\mu_2$ -bound oxygen atoms also contribute to the chelation of two adjacent zinc ions, and furthermore to the linkage of two dinuclear building blocks. In summary, all four

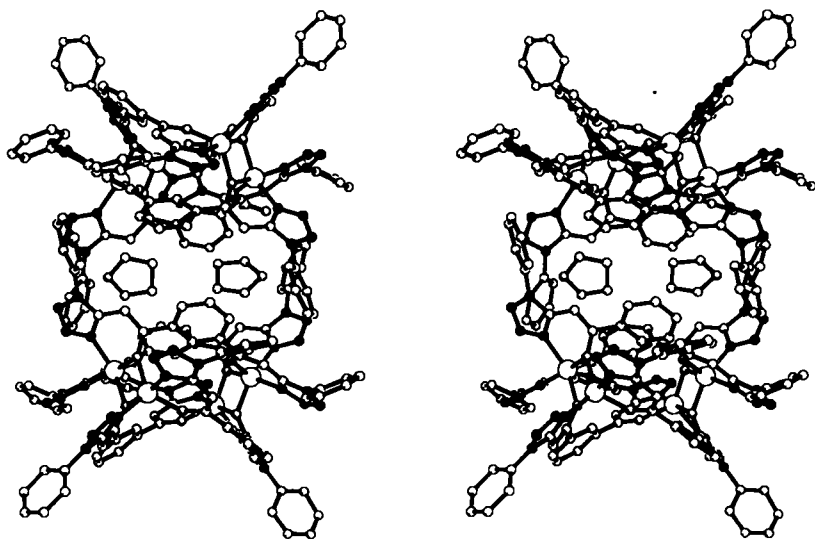
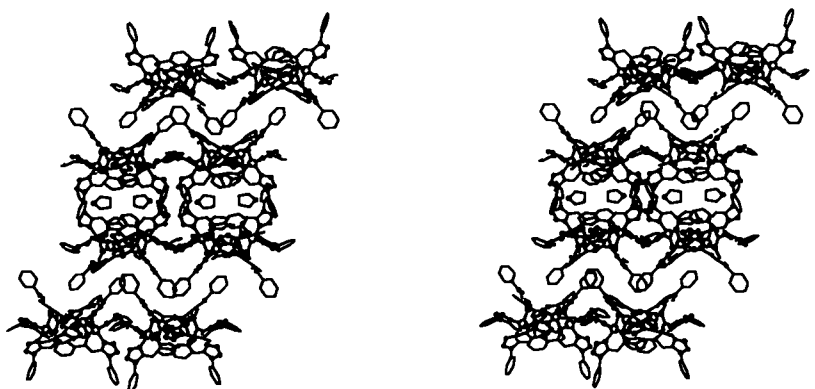
zinc ions in **10** are pentacoordinated and coordinatively saturated. A consequence of this steric arrangement is a metal-metal separation of ca. 324 pm. In contrast, the Zn-O-Zn-O- faces are separated by ca. 652 pm. The depiction of complex **10** here represents only one enantiomer of the racemic mixture obtained. It is noteworthy that the enantiomeric, tetranuclear (*P*-) and (*M*-)bis(double helicates) **10** (Fig. 1) are composed of two self-complementary, homochiral,<sup>[10]</sup> double-helical substructures [ $Zn_2L_3^2$ ]. As a result, in the crystal each dissymmetric enantiomer has approximately the high symmetry point group  $D_2$ , characterized by three  $C_2$  axes.

Initial evidence for the pairwise aggregation of bis(double helicate) **10**, leading to the cryptatoclathrate  $(10)_2 \cdot 2 THF$ ,<sup>[11]</sup> came from FAB MS. Apart from the molecular ion peak of **10**, the spectrum shows an additional peak of minor intensity at double this *m/e* (see experimental part). Detailed investigations of the X-ray crystallographic data of **10**, obtained from a single crystal grown in THF covered with a layer of diethylether, confirmed this assumption. Accordingly, **10** exists in the crystal as a  $D_2$  symmetric cryptatoclathrate  $(10)_2 \cdot 2 THF$  (stereo diagram, Fig. 3). The cavity that acts as host to two THF molecules is generated by two identical overlapping homochiral bis(double helicate) units **10**.<sup>[12]</sup> The unit cell consists of four clearly distinct cryptatoclathrate aggregates containing embedded THF molecules (Fig. 4). The supramolecular superstructure  $(10)_2 \cdot 2 THF$  exists because of van der Waals forces and is an example of *crystal engineering*.<sup>[6a]</sup>

In order to investigate whether the cryptatoclathrate  $(10)_2 \cdot 2 THF$  remains intact in solution or dissociates under these conditions, we carried out extensive  $^1H$  and  $^{13}C$  NMR studies. The uncoordinated ligand  $L^3$  has  $C_{2v}$  symmetry and, as expected, shows only one set of signals in the  $^1H$  and  $^{13}C$  NMR

Table 1. Selected distances (pm) and angles ( $^{\circ}$ ) in **10**.

Zn(1)–O(1)	193.7(4)	Zn(1)–O(3)	210.7(4)	Zn(1)–O(7)	203.3(4)
Zn(1)–N(1)	205.5(5)	Zn(1)–N(9)	204.9(5)	Zn(4)–O(3)	203.6(5)
Zn(4)–O(6)	193.5(4)	Zn(4)–O(7)	206.2(4)	Zn(4)–N(21)	204.3(5)
Zn(4)–N(25)	208.6(6)	Zn(1)–Zn(4)	324.3		
Zn(1)–O(7)–Zn(4)	104.8(2)	Zn(4)–O(3)–Zn(1)	103.0(2)	O(3)–Zn(4)–O(7)	76.5(2)
O(3)–Zn(4)–N(21)	97.8(2)	O(3)–Zn(4)–N(25)	136.5(2)	O(6)–Zn(4)–O(3)	111.7(2)
O(6)–Zn(4)–N(21)	92.5(2)	O(6)–Zn(4)–N(25)	110.1(2)	O(6)–Zn(4)–O(7)	104.8(2)
O(7)–Zn(4)–N(25)	81.8(2)	N(21)–Zn(4)–N(25)	91.9(2)	N(21)–Zn(4)–O(7)	162.7(2)
O(1)–Zn(1)–O(7)	118.3(2)	O(7)–Zn(1)–N(9)	122.1(2)	O(7)–Zn(1)–O(3)	75.5(2)
O(1)–Zn(1)–O(3)	95.8(2)	N(9)–Zn(1)–O(3)	82.3(2)	O(7)–Zn(1)–N(1)	100.0(2)
O(1)–Zn(1)–N(9)	116.6(2)	O(1)–Zn(1)–N(1)	90.2(2)	N(1)–Zn(1)–O(3)	173.7(2)
N(9)–Zn(1)–N(1)	96.7(2)				
Zn(3)–O(4)	201.6(6)	Zn(3)–O(2)	216.1(6)	Zn(3)–O(5)	193.6(6)
Zn(3)–N(13)	204.0(13)	Zn(3)–N(5)	204.0(11)	Zn(2)–O(2)	203.6(5)
Zn(2)–O(8)	193.2(5)	Zn(2)–O(5)	205.4(5)	Zn(2)–N(29)	202.8(6)
Zn(2)–N(17)	210.3(8)	Zn(3)–Zn(2)	319.3		
Zn(3)–O(5)–Zn(2)	106.3(3)	Zn(2)–O(2)–Zn(3)	99.0(2)	O(2)–Zn(2)–O(5)	77.3(2)
O(5)–Zn(3)–O(2)	77.0(3)	N(5)–Zn(3)–O(2)	79.8(4)	O(4)–Zn(3)–O(2)	91.3(2)
N(13)–Zn(3)–O(2)	175.5(4)	O(4)–Zn(3)–N(13)	93.1(4)	O(5)–Zn(3)–N(13)	101.5(4)
N(5)–Zn(3)–N(13)	97.8(5)	O(4)–Zn(3)–N(5)	111.4(4)	O(5)–Zn(3)–N(5)	123.4(4)
O(5)–Zn(3)–O(4)	119.9(3)	O(5)–Zn(2)–N(17)	83.8(3)	O(8)–Zn(2)–O(5)	103.0(2)
N(29)–Zn(2)–O(5)	163.9(2)	O(8)–Zn(2)–N(29)	93.1(2)	N(29)–Zn(2)–O(2)	96.9(2)
O(8)–Zn(2)–N(17)	107.3(3)	N(29)–Zn(2)–N(17)	91.9(3)	O(2)–Zn(2)–N(17)	140.7(3)
O(8)–Zn(2)–O(2)	110.3(2)				

Fig. 3. Stereoview of the crystal structure of  $(10)_2 \cdot 2$  THF (H atoms omitted, view along the crystallographic  $b$  axis) (PLUTON [17]).Fig. 4. Stereoview of the crystal packing of  $(10)_2 \cdot 2$  THF (view along the crystallographic  $b$  axis; H atoms omitted). For reasons of clarity only THF guest molecules encapsulated within the host cavity of  $(10)_2 \cdot 2$  THF are shown. The enantiomers of the homochiral superstructures  $(10)_2 \cdot 2$  THF alternate in the crystal.

spectrum. In contrast, crystalline samples of  $(10)_2 \cdot 2$  THF dissolved in  $\text{CDCl}_3$ ,  $[\text{D}_8]\text{THF}$  or  $\text{C}_6\text{D}_6$  do not show the expected signal patterns. If  $(10)_2 \cdot 2$  THF remained intact in solution, a total of four sets of signals for the positions present pairwise in ligand  $\text{L}^3$  should be expected. Instead, the solution spectra show only two signal sets (Fig. 5). This may be explained by the fact that  $(10)_2 \cdot 2$  THF dissociates in solution to give the tetranuclear unit  $[\text{Zn}_4\text{L}_2^3] (10)$ . In **10** the two halves of the ligands  $\text{L}^3$  are diastereotopic, owing to  $D_2$  molecular symmetry. Hence, the spectroscopic findings prove that the supramolecular superstructure  $(10)_2 \cdot 2$  THF must dissociate into two subunits **10** in the solvents used; **10** itself remains intact in solution as a tetranuclear complex. Even at elevated temperatures, no exchange phenomena were observed by NMR spectroscopy. Signal assignment of the  $^1\text{H}$  and  $^{13}\text{C}$  NMR spectra was achieved by means of a field gradient heteronuclear multiple-quantum coherence NMR (FG-HMQC) spectrum (Fig. 5). Further spectroscopic assignment of the diastereotopic ligand sites is not trivial. Application of additional methods based on NOE gave ambiguous results. This is a result of the pairwise similarity of interatomic distances. Interaction of solvent molecules ( $[\text{D}_8]\text{THF}$ ) with the protons of ligand  $\text{L}^3$  was detected by heteronuclear Overhauser spectroscopy ( $^1\text{H}$ ,  $^2\text{H}$  HOESY). Here, crosspeaks are detected between the  $^2\text{H}$  resonance lines of the bulk solvent and appropriate  $^1\text{H}$  resonance lines of **10**. Interestingly, one crosspeak involves the inward-directed H(3) protons. This suggests a weak penetration of solvent molecules into the cavity of **10**. Compared with the spectrum in solution, the solid-state  $^{13}\text{C}$  CP/MAS TOSS

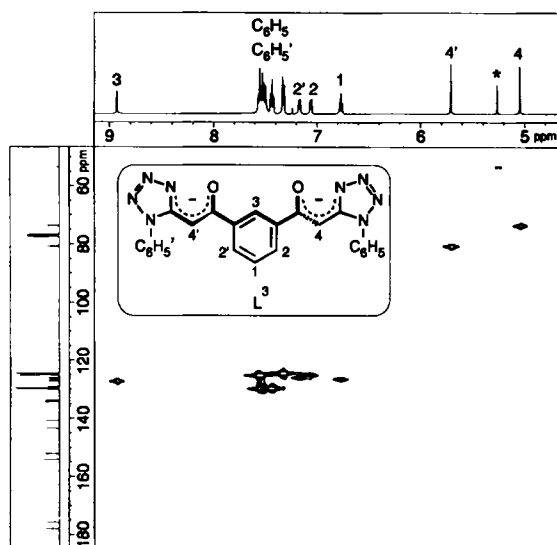


Fig. 5. Field gradient HMQC spectrum of  $(10)_2 \cdot 2\text{THF}$ ; crystals containing THF dissolved in  $\text{CDCl}_3$ ; +23 °C. \*:  $\text{CH}_2\text{Cl}_2$  from the preparation of crystals. The  $^1\text{H}$  and  $^{13}\text{C}$  range of THF signals has been omitted. The diastereotopicity within ligand  $L^3$  results from its coordination to the metal centres.

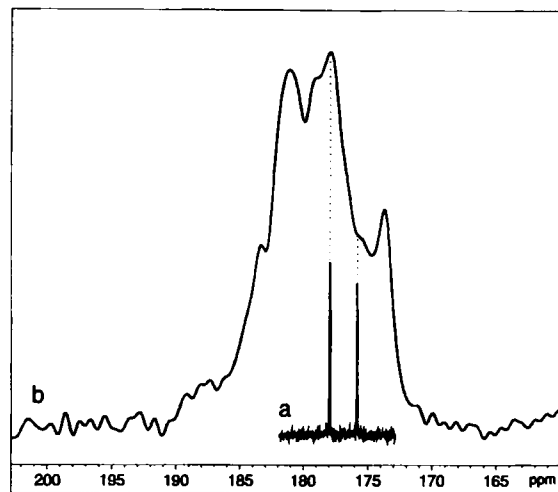


Fig. 6. Spectrum a: Part of the  $^{13}\text{C}$  NMR spectrum of  $(10)_2 \cdot 2\text{THF}$ ; dissolved crystals in  $\text{CDCl}_3$ . Owing to the diastereotopicity within a coordinated ligand two signals are detected in the carbonyl range. Spectrum b: Part of the  $^{13}\text{C}$  CP/MAS TOSS solid-state spectrum of  $(10)_2 \cdot 2\text{THF}$ . As a result of the crystal geometry the spectrum is further split in the carbonyl range in comparison to spectrum a.

spectrum of  $(10)_2 \cdot 2\text{THF}$  (Fig. 6) shows further splitting. This finding is in agreement with the structure of cryptatoclathrate  $(10)_2 \cdot 2\text{THF}$ , found by X-ray analysis. By comparison, Figure 6 shows the carbonyl  $^{13}\text{C}$  NMR signals of dissolved crystals of  $(10)_2 \cdot 2\text{THF}$ , along with  $(10)_2 \cdot 2\text{THF}$  in the solid state. The higher number of signals in the solid state is obvious.

## Conclusions

Ligand **7** combines the good complex-building properties of **1** towards iron(III) ions with the geometry (1,4-phenylene spacer) of ligand **5**, leading to  $[\text{Fe}_4\text{L}_6^1]$  (**6**). We have shown that **7** yields tetranuclear chelate complexes  $[\text{Fe}_4\text{L}_6^2]$  (**8**) as well. As a consequence we wanted to learn about the impact of geometric changes (1,4- versus 1,3-phenylene spacer) on the complex-building properties of the bridging ligands, as realised in doubly

deprotonated **9**. Although the formation of bis(double helicate) **10** and cryptatoclathrate  $(10)_2 \cdot 2\text{THF}$  was rather fortuitous, further experiments will permit predictions concerning possible supramolecular structures of the products created from bridging ligands  $L^1$ ,  $L^2$  and  $L^3$  along with appropriate metal cations.

## Experimental Procedure

**Materials and methods:** All preparations were carried out under an atmosphere of dry nitrogen. All common reagents and solvents were purchased from commercial suppliers and used without further purification unless otherwise indicated. *N,N*-Dimethylformamide was distilled from  $\text{P}_2\text{O}_5$  under dry nitrogen and stored over 4 Å molecular sieves. Sodium hydride (80% dispersion in mineral oil) was purchased from Aldrich. Melting points were determined on a Wagner & Munz apparatus and are uncorrected. Infrared spectra were recorded on a Beckman Acculab or a Perkin-Elmer 1420 Ratio-Recording Infrared Spectrophotometer.  $^1\text{H}$  NMR spectra were recorded on a Jeol JNM-PMX-60 (60 MHz) or JNM-GX-400 spectrometer (400 MHz).  $^{13}\text{C}$  NMR spectra were recorded on a Jeol JNM-GX-400 spectrometer (100 MHz). Carbon atom type assignment was achieved by the DEPT technique.  $^1\text{H}$ ,  $^{13}\text{C}$  2D HMQC spectra and  $^{13}\text{C}$  CP/MAS TOSS spectra were recorded on a Jeol Alpha 500 spectrometer (500 MHz, for  $^1\text{H}$ ). All chemical shifts are based on the  $\delta$  scale with TMS as an internal standard. Mass spectra were recorded on a Varian MAT 3rA (EIMS) or on a Finnigan MAT TSQ 70 spectrometer ( $m/z \leq 1500$ ; ion source temperature: 50 °C; ion desorption from *m*-NBA matrix: 10 keV xenon atoms, FABMS) or on a Finnigan MAT 711 A (AMD Intetra modified,  $m/z > 1500$ , ion source temperature: 35 °C, ion desorption: 12 keV  $\text{Cs}^+$  ions, LSIMS). Elemental analyses were carried out on a Heraeus CHN-Mikroautomat or by I. Betz Microanalytical Laboratory, Kronach (Germany).

**1,3-Bis[1-(1-phenyl-1H-tetrazol-5-yl)ethan-2-one]benzene (9):** Compound **9** was prepared in the following two stages.

**1,3-Bis(3-anilino-3-methylthiopropen-1-one)benzene (Bis(ketene-*N,S*-acetal)) [13]:** A solution of 1,3-diacetylbenzene (8.11 g, 50 mmol) in absolute DMF (90 mL) was added dropwise with stirring to a suspension of sodium hydride (3.0 g, 100 mmol) in absolute DMF (160 mL) at an ice-bath temperature of 0 °C. After the addition was completed, stirring was continued at room temperature. A solution of phenylisothiocyanate (13.51 g, 100 mmol) in absolute DMF (30 mL) was then added dropwise. After stirring for 4 h, the reaction mixture was cooled to 10 °C and methyl iodide (14.20 g, 100 mmol) was added dropwise. Stirring was continued at room temperature for 16 h. The reaction mixture was poured into ice water (1 L) and the resulting precipitate was filtered off, washed with water and extracted into  $\text{CH}_2\text{Cl}_2$  (200 mL). The organic layer was washed with water (3 × 200 mL), dried ( $\text{MgSO}_4$ ) and filtered. The solvent was removed in vacuo and the residue was recrystallized from  $\text{CHCl}_3/\text{Et}_2\text{O}$  (2:1) to afford 10.6 g (46%) of the desired product as a yellow crystalline material. M.p. 157 °C;  $^1\text{H}$  NMR (400 MHz,  $\text{CDCl}_3$ , 25 °C):  $\delta$  = 2.46 (s, 6H;  $\text{SCH}_3$ ), 5.95 (s, 2H; =CH), 7.24–7.41 (m, 10H;  $\text{C}_6\text{H}_5$ ), 7.52 (t,  $^3J(\text{H,H}) = 7.7$  Hz, 1H;  $\text{C}_6\text{H}_4$  (5)), 8.01 (d,  $^3J(\text{H,H}) = 7.7$  Hz, 2H;  $\text{C}_6\text{H}_4$  (4,6)), 8.42 (s, 1H;  $\text{C}_6\text{H}_4$  (2)), 13.52 (s, 2H; NH); IR (KBr):  $\tilde{\nu} = 1550 \text{ cm}^{-1}$  (C=O); MS (70 eV, EI):  $m/z$  (%): 460 (27.1) [ $M^+$ ].

**Bistetrazole 9 [13]:** To a stirred solution of bis(ketene-*N,S*-acetal) (10.6 g, 23 mmol) in  $\text{CH}_3\text{CN}$  (180 mL), a solution of  $\text{NaN}_3$  (3.0 g, 46 mmol) in DMSO (90 mL) was added dropwise at 100 °C. The stirred reaction mixture was heated under reflux for 4 d until a clear solution occurred. It was then cooled to room temperature, poured into crushed ice (1000 g) and acidified with 20% acetic acid (pH = 5), and the precipitate was filtered off, washed with water and redissolved in  $\text{CH}_2\text{Cl}_2$  (300 mL). The organic layer was washed with water (3 × 300 mL), dried ( $\text{MgSO}_4$ ) and evaporated in vacuo. The resulting solid was recrystallized from  $\text{CH}_2\text{Cl}_2/\text{Et}_2\text{O}$  (2:1) affording the title compound as a white powder (8.8 g, 85%). M.p. 190 °C;  $^1\text{H}$  NMR (400 MHz,  $[\text{D}_6]\text{DMSO}$ , 25 °C):  $\delta$  = 5.20 (s, 4H;  $\text{CH}_2$ ), 7.56–7.64 (m, 10H;  $\text{C}_6\text{H}_5$ ), 7.70 (t,  $^3J(\text{H,H}) = 7.9$  Hz, 1H;  $\text{C}_6\text{H}_4$ ), 8.21 (d,  $^3J(\text{H,H}) = 7.9$  Hz, 2H;  $\text{C}_6\text{H}_4$ ), 8.47 (s, 1H;  $\text{C}_6\text{H}_4$ );  $^{13}\text{C}$  NMR (100.5 MHz,  $[\text{D}_6]\text{DMSO}$ , 25 °C):  $\delta$  = 34.47 (2  $\text{CH}_2$ ), 124.77, 128.40, 129.55, 129.90, 130.46, 133.51, 135.43 (18 Ar-C, two signals coincide), 150.64 (2 C=N), 192.96 (2 C=O); IR (KBr):  $\tilde{\nu} = 1680 \text{ cm}^{-1}$  (C=O), 1590, 1490 (C=C, C=N, N=N); MS (70 eV, EI):  $m/z$  (%): 450 [ $M^+$ ];  $\text{C}_{24}\text{H}_{18}\text{N}_8\text{O}_2$  (450.46); calcd C 63.99, H 4.03, N 24.88; found C 64.07, H 4.37, N 24.95.

**Tetrakis[2,2'-(1-phenyl-1H-tetrazol-5-yl)-1,1'-(1,3-benzenediyl)]bis(ethen-1-olato)-(2-)-*O,N'*; $\mu$ -*O,N''*]tetrazine(II) (10):** To a solution of  $\text{Zn}(\text{OAc})_2 \cdot 2\text{H}_2\text{O}$  (0.165 g, 0.75 mmol) in methanol (50 mL), a solution of bistetrazole **9** (0.338 g, 0.75 mmol) in  $\text{CH}_2\text{Cl}_2$  (25 mL) was added. The mixture was stirred for 16 h, filtered under suction, then the residue was washed with  $\text{CH}_3\text{OH}$  (20 mL) and  $\text{Et}_2\text{O}$  (20 mL), and dried in vacuo to afford 0.284 g (74%) of **10** as a white powder. M.p. > 300 °C (decomp.);  $^1\text{H}$  NMR (400 MHz,  $\text{CDCl}_3$ , 25 °C):  $\delta$  = 5.05 (s, 4H; =CH), 5.72 (s, 4H; =CH), 6.78 (t,  $^3J(\text{H,H}) = 7.6$  Hz, 4H;  $\text{C}_6\text{H}_4$ ), 7.06 (d,  $^3J(\text{H,H}) = 7.6$  Hz, 4H;  $\text{C}_6\text{H}_4$ ), 7.16 (d,  $^3J(\text{H,H}) = 7.6$  Hz, 4H;  $\text{C}_6\text{H}_4$ ), 7.32–7.57 (m, 40H;  $\text{C}_6\text{H}_5$ ), 8.94 (s, 4H;  $\text{C}_6\text{H}_4$ );  $^{13}\text{C}$  NMR (100.5 MHz,  $\text{CDCl}_3$ , 25 °C):  $\delta$  = 73.81 (4 =CH), 80.78

(4=CH), 124.54, 125.14, 126.00, 126.59, 127.30, 129.16, 129.53, 129.82, 130.11 (56 Ar-CH, two signals coincide), 133.71 (4 Ar-C<sub>q</sub>), 134.28 (4 Ar-C<sub>q</sub>), 140.76 (4 Ar-CN), 143.49 (4 Ar-CN), 152.13 (4 C≡N), 154.16 (4 C≡N), 175.81 (4 C≡O), 177.96 (4 C≡O); IR (KBr):  $\tilde{\nu}$  = 1590, 1530, 1490 cm<sup>-1</sup> (C=N, C=C, N=N); MS (FAB):  $m/z$  = 1028.6 [Zn<sub>2</sub>L<sub>2</sub><sup>+</sup> + H]<sup>+</sup>, 2055.9 [M + H]<sup>+</sup>, 4110.2 [M<sub>2</sub>]<sup>+</sup>; C<sub>66</sub>H<sub>44</sub>N<sub>12</sub>O<sub>8</sub>Zn<sub>4</sub> (2055.34): calcd C 56.10, H 3.14, N 21.81, Zn 12.72; found C 55.26, H 3.51, N 21.80, Zn 11.83.

**X-ray structure analysis:** Crystals suitable for X-ray structure analysis were obtained by diffusion of Et<sub>2</sub>O into a THF solution of **10**. Crystal data for **10**: C<sub>66</sub>H<sub>44</sub>N<sub>12</sub>O<sub>8</sub>Zn<sub>4</sub> + 5 C<sub>4</sub>H<sub>8</sub>O,  $M_r$  = 2055.34 + 5 × 72.11, monoclinic, space group C2/c,  $a$  = 4567.6(9),  $b$  = 1854.9(4) and  $c$  = 2732.2(6) pm,  $\beta$  = 106.63(3)°,  $V$  = 22.180(8) nm<sup>3</sup>,  $Z$  = 8,  $\rho$  (calcd.) = 1.447 Mg m<sup>-3</sup>,  $F(000)$  = 9984,  $\lambda$  = 71.073 pm,  $T$  = 153 K,  $\mu(\text{MoK}\alpha)$  = 0.934 mm<sup>-1</sup>. Crystal dimensions: 0.7 × 0.6 × 0.6 mm. The data were collected on a Stoe–Siemens–Huber diffractometer. Intensity determinations were performed on a shock-cooled crystal in an oil drop [14] according to the  $2\theta/\omega$  method in the region 8° ≤ 2θ ≤ 45°. Of the 14817 collected reflections, 14520 were unique, and of these 14519 were used for refinement of 2107 parameters by means of 2630 restraints. During structure refinement the analysis of the Zn(3) anisotropic displacement parameters indicated the disorder of that atom over two sites within the O(2)–Zn(2)–O(5) plane and orthogonal to the O(2)–Zn(2)–O(5) bisection. The site occupation factors were refined to 0.65 and 0.35, respectively. As a consequence particularly those ligands coordinated to Zn(3) in the Zn(2)/Zn(3) hemisphere of the complex are heavily disordered. The tetrazole ring containing N(5)–N(8) is disordered over three positions as well as the phenyl ring connected to that moiety (C(19)–C(24)). The Zn(3) bonded ligands containing N(13)–N(16) and N(17)–N(20) and the related phenyl rings are only disordered over two sites. Ligand as well as THF lattice molecule disorder was successfully modelled by employing 1,2-, 1,3-distance- and ADP-similarity restraints. Highest minima and maxima: 726 and –469 enm<sup>-3</sup>, respectively.  $R1(I > 2\sigma(I))$  = 0.0708 and  $wR2$  = 0.1971 (all data),  $R1 = \sum ||F_o| - |F_c|| / \sum |F_o|$ ,  $wR2 = [\sum w(F_o^2 - F_c^2)^2 / \sum w(F_c^2)^2]^{0.5}$ . The structure was solved by direct methods (SHELXS 90) [15] and refined on  $F^2$  by means of the full-matrix least-squares method (SHELXL 93) [16]. Crystallographic data (excluding structure factors) for the structure reported in this paper have been deposited with the Cambridge Crystallographic Data Centre as supplementary publication no. CCDC-1220-29. Copies of the data may be obtained free of charge on application to The Director, CCDC, 12 Union Road, Cambridge CB2 1EZ, UK (Fax: Int. code + (1223) 336-033; e-mail: teched@chemcrs.cam.ac.uk).

**Acknowledgements:** This work was supported by the Deutsche Forschungsgemeinschaft and the Fonds der Chemischen Industrie. R. W. S. is grateful to Prof. Dr. R. Snaith, Department of Chemistry, University of Cambridge, and to St John's College for an Overseas Visiting Scholarship, Easter Term 1995. Initial ideas concerning this work formed during this period.

Received: March 27, 1996 [F 336]

- [1] R. W. Saalfrank, C.-J. Lurz, K. Schobert, O. Struck, E. Bill, A. X. Trautwein, *Angew. Chem.* **1991**, *103*, 1499–1501; *Angew. Chem. Int. Ed. Engl.* **1991**, *30*, 1494–1496.
- [2] a) R. W. Saalfrank, O. Struck, K. Nunn, C.-J. Lurz, R. Harbig, K. Peters, H. G. von Schnering, E. Bill, A. X. Trautwein, *Chem. Ber.* **1992**, *125*, 2331–2335; b) R. W. Saalfrank, O. Struck, K. Peters, H. G. von Schnering, *Chem. Ber.* **1993**, *126*, 837–840.
- [3] R. W. Saalfrank, B. Hörner, D. Stalke, *Angew. Chem.* **1993**, *105*, 1223–1225; *Angew. Chem. Int. Ed. Engl.* **1993**, *32*, 1179–1182.
- [4] R. W. Saalfrank, R. Burak, S. Reihls, N. Löw, F. Hampel, H.-D. Stachel, L. Lentmaier, K. Peters, E.-M. Peters, H. G. von Schnering, *Angew. Chem.* **1995**, *107*, 1085–1087; *Angew. Chem. Int. Ed. Engl.* **1995**, *35*, 993–995.
- [5] R. Harbig, thesis, University of Erlangen-Nürnberg (Germany), **1996**.
- [6] a) P. N. W. Baxter, J.-M. Lehn, J. Fischer, M.-T. Youinou, *Angew. Chem.* **1994**, *106*, 2432–2434; *Angew. Chem. Int. Ed. Engl.* **1994**, *33*, 2284–2287; b) J.-M. Lehn, *Angew. Chem.* **1988**, *100*, 91–116; *Angew. Chem. Int. Ed. Engl.* **1988**, *27*, 89–112; c) J.-M. Lehn, *Angew. Chem.* **1990**, *102*, 1347–1362; *Angew. Chem. Int. Ed. Engl.* **1990**, *29*, 1304–1319; d) J. S. Lindsey, *New J. Chem.* **1991**, *15*, 153–180; e) G. M. Whitesides, J. P. Mathias, C. T. Seto, *Science* **1991**, *254*, 1312–1319; f) D. Philp, J. F. Stoddart, *Angew. Chem.* **1996**, *108*, 1242–1286; *Angew. Chem. Int. Ed. Engl.* **1996**, *35*, 1154–1196; g) G. R. Desiraju, *Angew. Chem.* **1995**, *107*, 2541–2558; *Angew. Chem. Int. Ed. Engl.* **1995**, *34*, 2311–2327.
- [7] [Fe<sub>2</sub>L<sub>3</sub>]: Elemental analyses C<sub>72</sub>H<sub>48</sub>N<sub>24</sub>O<sub>6</sub>Fe<sub>2</sub> (1457.02): calcd C 59.35, H 3.32, N 23.07, Fe 7.67; found C 59.39, H 3.50, N 22.84, Fe 7.13; IR (KBr):  $\tilde{\nu}$  = 3400 cm<sup>-1</sup> (OH); 1540, 1530, 1500 (C=N, C=C, N=N); MS (FAB):  $m/z$ : 1475.4 [Fe<sub>2</sub>L<sub>3</sub>·H<sub>2</sub>O + H]<sup>+</sup>, 1457.4 [Fe<sub>2</sub>L<sub>3</sub> + H]<sup>+</sup>. Examination of a CPK molecular model of [Fe<sub>2</sub>L<sub>3</sub>] indicates a triple helicate with D<sub>3</sub> symmetry and (Δ,Δ)-(Λ,Λ)-fac configuration at the octahedral iron(III) centres. An X-ray structure analysis is being carried out.
- [8] See also: a) *Frontiers in Supramolecular Organic Chemistry and Photochemistry* (Eds.: H.-J. Schneider, H. Dürr), VCH, Weinheim, **1991**; b) C. Seel, F. Vögtle, *Angew. Chem.* **1992**, *104*, 542–563; *Angew. Chem. Int. Ed. Engl.* **1992**, *31*, 528–549; c) P. Timmerman, W. Verboom, F. C. J. M. van Veggel, J. P. M. van Duynhoven, D. N. Reinhoudt, *Angew. Chem.* **1994**, *106*, 2437–2440; *Angew. Chem. Int. Ed. Engl.* **1994**, *33*, 2345–2348.
- [9] For further examples see: a) R. Krämer, J.-M. Lehn, A. De Cian, J. Fischer, *Angew. Chem.* **1993**, *105*, 764–767; *Angew. Chem. Int. Ed. Engl.* **1993**, *32*, 703–706; b) E. C. Constable, *Tetrahedron* **1992**, *48*, 10013–10059.
- [10] a) D. Sellmann, H. Friedrich, F. Knoch, *Z. Naturforsch.* **1993**, *48 b*, 1675–1680; b) F. A. L. Anet, S. S. Miura, J. Siegel, K. Mislow, *J. Am. Chem. Soc.* **1983**, *105*, 1419–1426.
- [11] For the classification and nomenclature of host–guest-type compounds, see: a) E. Weber, H.-P. Josel, *J. Incl. Phenom.* **1983**, *1*, 79–85; b) E. Weber in *Topics in Current Chemistry*, Vol. 140 (Eds.: M. J. S. Dewar, J. D. Dunitz, K. Hafner, E. Heilbronner, S. Ito, J.-M. Lehn, K. Niedenzu, K. N. Raymond, C. W. Rees, F. Vögtle, G. Wittig), Springer, Berlin, **1987**, p. 14 ff.
- [12] For recent studies on inclusion compound chemistry, see: a) C. D. Gutsche in *Calixarenes* (Ed.: J. F. Stoddart), Royal Society of Chemistry, Cambridge, **1992**, ch. 6, p. 149 ff; b) R. Ungaro, A. Pochini, G. D. Andreatti, P. Domiano, *J. Chem. Soc. Perkin Trans. II* **1985**, 197–201; c) P. Timmerman, K. G. A. Nierop, E. A. Brinks, W. Verboom, F. C. J. M. van Veggel, W. P. van Hoorn, D. N. Reinhoudt, *Chem. Eur. J.* **1995**, *1*, 132–143; d) M. Perrin, F. Gharnati, D. Oehler, R. Perrin, S. Lecocq, *J. Inclusion Phenom.* **1992**, *14*, 257–270; e) D. J. Cram, J. M. Cram in *Container Molecules and Their Guests* (Ed.: J. F. Stoddart), Royal Society of Chemistry, Cambridge, **1994**, ch. 6, p. 107 ff; f) D. J. Cram, H.-J. Choi, J. A. Bryant, C. B. Knobler, *J. Am. Chem. Soc.* **1992**, *114*, 7748–7765; g) C. Valdés, U. P. Spitz, S. W. Kubik, J. Rebek, Jr., *Angew. Chem.* **1995**, *107*, 2031–2033; *Angew. Chem. Int. Ed. Engl.* **1995**, *34*, 1885–1887.
- [13] a) R. T. Chakrasali, H. Ila, H. Junjappa, *Synthesis* **1988**, 453–455; b) A. Kumar, V. Aggarwal, H. Junjappa, *Synthesis* **1980**, 748–751; c) W. D. Rudolf, A. Schierhorn, M. Augustin, *Tetrahedron* **1979**, *35*, 551–556; d) R. Gompper, H. Schaefer, *Chem. Ber.* **1967**, *100*, 591–604.
- [14] T. Kottke, D. Stalke, *J. Appl. Crystallogr.* **1993**, *26*, 615–619.
- [15] G. M. Sheldrick, *Acta Crystallogr. Sect. A* **1990**, *46*, 467–473.
- [16] G. M. Sheldrick, SHELXL 93, University of Göttingen, **1993**.
- [17] a) A. L. Spek, PLUTON93 graphics program, University of Utrecht, **1993**; b) A. L. Spek, *Acta Crystallogr. Sect. A* **1990**, *46*, C34.